

much more general feature of the $A \approx 200$ transitional region than existing γ -spectroscopy data indicate. The $\langle M_K \rangle$ measurements and our nuclear structure inferences are described in detail in two recent publications.^{2,3}

- 1) S.E. Vigdor et al., IUCF Scientific and Technical Report 1980, p. 108.
- 2) H.J. Karwowski et al., Phys. Rev. Lett. 47, 1251 (1981).
- 3) H.J. Karwowski et al., Phys. Rev. C, in press (IUCF preprint no. 171).
- 4) J. Kropp et al., Z. Phys. A280, 61 (1977).

THE INFLUENCE OF DEFORMED-NUCLEUS LEVEL DENSITIES ON STATISTICAL MODEL CALCULATIONS FOR HIGH-SPIN FISSION

S.E. Vigdor and H.J. Karwowski
Indiana University Cyclotron Facility, Bloomington, Indiana 47405

During the past year we have continued our investigation¹⁻⁴ of fission and particle emission from hot, high-spin nuclei by making substantial further improvements in the statistical model analysis of such data. We have specifically incorporated methods for estimating the effects of (1) the expected dilution of collective rotational bands with increasing temperature on the level densities for deformed nuclei, and (2) the deformation of daughter nuclei on the barrier transmission coefficients for particle emission. In the process of introducing the latter change, we also found and corrected a significant long-standing error in the widely used optical model subroutine TLJ. With these and the numerous other improvements we have introduced over the past few years (see refs. 1-4), our statistical model code now differs extensively from its progenitor MB-II (ref. 5), and we have renamed the Indiana version MBEGAT.

We have previously stressed² the importance, for the sake of consistency in calculations of fission-evaporation competition, of generating level densities as a function of total angular momentum not by the conventional technique,⁵ which implicitly assumes spherical symmetry, but rather by the K -summation technique introduced for deformed nuclei by Bjornholm, Bohr, and Mottelson (BBM).⁶ In the latter approach,

collective rotational bands built upon every intrinsic nucleon configuration are included in the level density. For an axially symmetric nuclear shape characterized by moment of inertia \mathcal{J}_\perp with respect to an axis orthogonal to the symmetry axis, inclusion of the rotational bands enhances the intrinsic level densities at nuclear temperature τ by a factor $\mathcal{J}_\perp \tau / \hbar^2$. In our previous analysis of measurements of fission-evaporation competition following ${}^6\text{Li}$ -induced fusion reactions,^{2,3} we incorporated this collective enhancement of level densities at both the strongly prolate saddle-point deformations relevant to fission and the mildly oblate equilibrium deformations used in evaluating particle emission widths. We were able to reproduce very well the relative values of fission cross sections (σ_{fiss}) and anisotropies (γ_{fiss}) and α -evaporation cross sections (σ_α) measured for various targets and bombarding energies, without any adjustable parameters. [All nuclear structure properties needed for the calculations were fixed according to predictions of the rotating-liquid-drop (RLDM) and non-interacting Fermi gas (NIFG) models, see Refs. 2,3]. However, after allowance in the calculations for pre-equilibrium nucleon emission manifested in the observed proton energy spectra and (${}^6\text{Li}, xn$) residue mass distributions, the calculated absolute values

overestimated γ_{fiss} measurements by a factor 1.05-1.15, and underestimated σ_{α} by a factor ≈ 0.8 and σ_{fiss} by 0.5-0.6 (see Refs. 2,3).

In our most recent calculations we have addressed a questionable assumption underlying the BBM approach to deformed-nucleus level densities, namely, that of complete independence of the collective and intrinsic degrees of freedom. In a broad sense, this assumption is not valid, since all nuclear excitations can be accounted for in principle by intrinsic degrees of freedom alone. However, the collectivity does act to redistribute levels with respect to energy, giving rise to an effective separation between rotational and intrinsic motion at low temperatures. As stressed by BBM,⁶ this effective distinction must begin to fade at temperatures where the single-particle excitations which contribute coherently to the rotational motion would also contribute appreciably to the intrinsic level density. The relevant single-particle excitations are generated by the Coriolis coupling,⁶ and in an axially-symmetric harmonic oscillator well they fall predominantly at energies

$$\epsilon_{\text{Coriolis}} \sim \pm \hbar(\omega_2 - \omega_3) \sim (41 \text{ MeV}) A^{-1/3} |\delta_{\text{osc}}|. \quad (1)$$

In Eq. (1) ω_2 and ω_3 denote the oscillator frequencies for particle motion in the directions perpendicular to the rotation axis; their difference can be expressed as the product of the mean oscillator frequency ($\hbar\omega_0 \approx 41 A^{-1/3} \text{ MeV}$) and a potential deformation parameter⁶ δ_{osc} (positive for prolate and negative for oblate shapes).

In Fig. 1, we illustrate the effects on nuclear level densities of allowing a smooth transition from collectively enhanced values at temperatures small compared to $\epsilon_{\text{Coriolis}}$ to purely intrinsic densities for $\tau \gg \epsilon_{\text{Coriolis}}$. The broken curves in the figure are based on two different, somewhat arbitrary, analytical

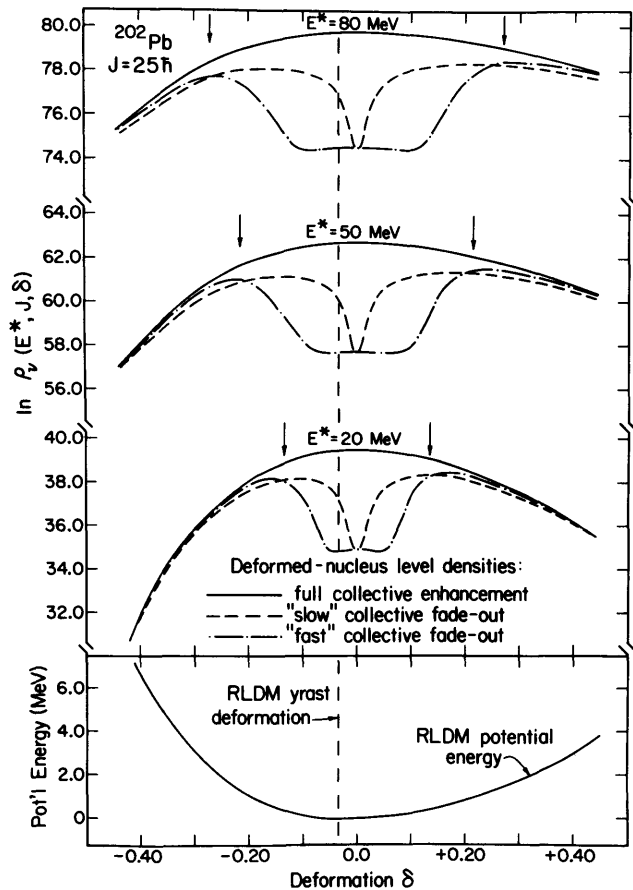


Figure 1. Illustration of the temperature-dependent shift in the most probable daughter-nucleus deformation when the collective level density enhancement is allowed to fade as the temperature approaches the single-particle Coriolis excitation of Eq. (1). The potential energy curve in the bottom frame is calculated for axially symmetric shapes in ^{202}Pb , at an angular momentum of $25\hbar$, using the approximate relations from ref. 4 and setting the energy to zero at spherical symmetry. The dashed vertical line marks the deformation corresponding to the minimum potential energy. In the top frame the logarithm of the level density is plotted vs. deformation for three excitation energies. The E^* - values are specified in the figure with respect to the potential energy of a rigid sphere, but in the level density calculations these values are decremented by the deformation energy for $\delta \neq 0$. The solid level density curves are calculated with eqs. (33) and (34) in ref. 4, while the broken curves include collective enhancement dilution functions specified in ref. 4. The vertical arrows indicate the oblate and prolate shapes corresponding to the cutoff deformation of eq. (2), with $\zeta=1.0$, for each excitation.

expressions for the fade-out of the collective enhancement (see ref. 4 for details). In both cases, and for all the excitation energies included in the figure, there is a very large reduction in level densities, from the values including the full collective enhancement, at small deformations, such as the RLDM yrast deformation for ^{202}Pb at $J=25\hbar$. In contrast, at the RLDM saddle-point deformation ($\delta \approx 1.0$) the full collective enhancement is still in effect. It is crucial for understanding the influence of the collective enhancement fade-out on calculations of fission-evaporation competition to recognize that the appropriate deformation to use in evaluating particle emission widths (short of a complete, but excessively time-consuming, integration over deformation) is the most probable one reached in the daughter nucleus. The calculations in Fig. 1 illustrate that this most probable deformation is likely to be significantly larger in magnitude than the yrast deformation (where the intrinsic level density is maximized). However, the peak value of the level density for the broken curves is still appreciably smaller (typically by a factor ~ 2) than the value for the solid curves at the yrast deformation, which was used in our earlier statistical model calculations. The net effect of the collective fade-out at the temperatures of interest to us is therefore to enhance fission with respect to particle evaporation by a factor which grows as the most probable deformation shifts further away from the RLDM yrast value ($\delta_{yr}^{\text{RLDM}}$) i.e., as the temperature increases for fixed spin of the daughter nucleus or as the spin (and hence $|\delta_{yr}^{\text{RLDM}}|$) decreases for fixed τ .

The above effects are incorporated approximately in our code⁴ by introducing a sharp cutoff in the collective enhancement of the level densities within a

given E^*-J bin of the appropriate daughter nucleus, at a cutoff deformation

$$|\delta_c| = \tau A^{1/3} / (41 \zeta \text{ MeV}). \quad (2)$$

The use of the adjustable (spin- and temperature-independent) normalization factor ζ provides some freedom to accommodate the quantitative uncertainties which exist in the precise location of the relevant Coriolis excitations and in their precise relation to the temperature scale characterizing the reduction in the collective enhancement. We expect ζ to be of order unity, but we have investigated the influence on our calculations of plausible variations in this parameter. We have also modified the code to take approximate account of the increased daughter-nucleus deformation in evaluating barrier transmission coefficients for particle emission, using a technique explained in ref. 4. The main effect of the deformed barriers is to enhance α -evaporation slightly with respect to nucleon emission.

We illustrate the influence of variations in ζ on the spin and chance distributions for fission in Fig. 2. In Fig. 3 we compare calculations for various decay properties of ^{203}Pb , formed in $^6\text{Li} + ^{197}\text{Au}$ fusion at a number of bombarding energies, for three different level density treatments: the conventional spherical treatment,⁵ our earlier treatment including full collective enhancement at all deformations, and the present treatment with $\zeta=1.0$. It can be seen that inclusion of the collective enhancement fade-out leads to an increase in calculated values of σ_{fiss} , a decrease in γ_{fiss} , and a slight increase in σ_{α} at the lower bombarding energies, in comparison with the full collective calculations. All of these changes are in the appropriate direction to improve the agreement

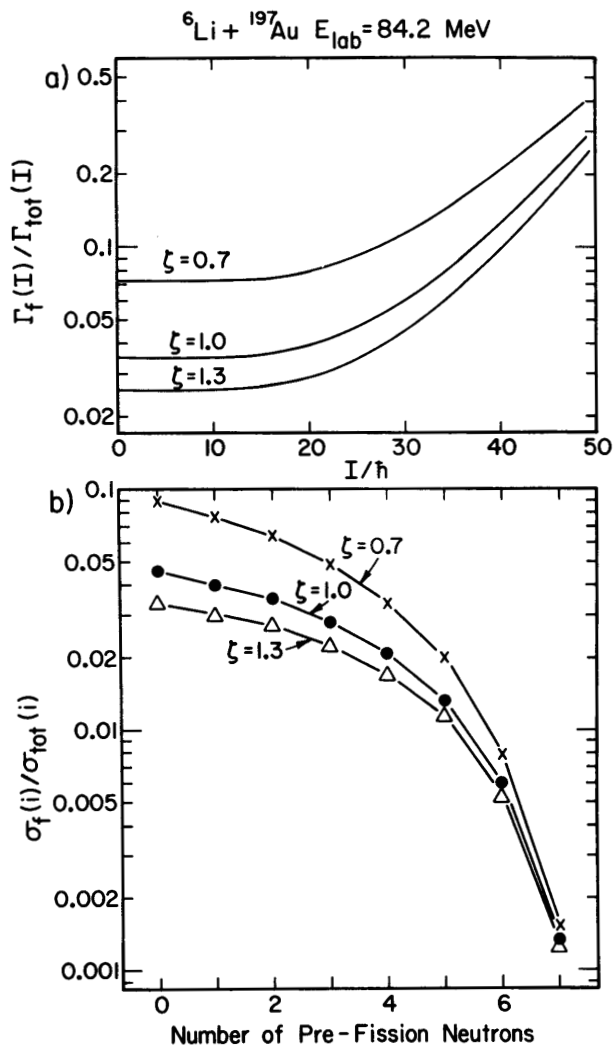


Figure 2. The (a) spin- and (b) chance-distributions for fission following fusion of 84.2 MeV ${}^6\text{Li} + {}^{197}\text{Au}$, from statistical model calculations incorporating the fade-out of the collective level density enhancement, for three different values of the cutoff deformation normalization parameter ζ . The relative partial width for 1st-chance fission is plotted vs. the compound-nucleus angular momentum in (a), while the spin-integrated relative fission cross section is plotted for the various stages of the decay chain in (b). With the exception of ζ , all input parameters are identical for the three calculations, with values given and justified in ref. 3.

between theory and our experimental results for ${}^6\text{Li}$ -induced fusion reactions. The overall magnitude of the fade-out effects (but not the relative effects on different decay properties) can be varied by adjusting the cutoff deformation normalization parameter ζ . In

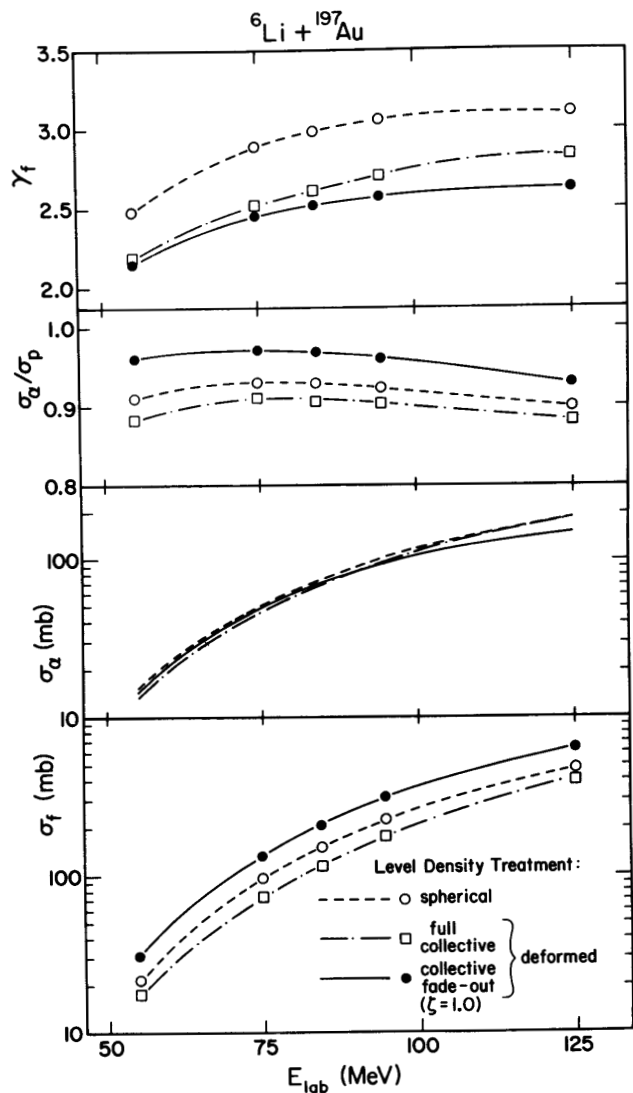


Figure 3. The influence of the level density treatment on calculated decay properties for ${}^6\text{Li} + {}^{197}\text{Au}$ as a function of bombarding energy. The quantities displayed are the total fission cross section (σ_{fiss}) and anisotropy (γ_{fiss}), the absolute cross section for α -evaporation (σ_α), and its ratio (σ_α/σ_p) to that for proton evaporation. The initial compound-nucleus spin distribution is based on an assumed total fusion cross section of 1100 mb at $E_{lab} = 55$ MeV and 1213 mb (an average of measured values³ for various targets and energies) at all higher energies.

Fig. 4 we show that with ζ adjusted to 1.05 (a physically very reasonable value), our most complete calculations (including also a "hot-spot" simulation of pre-equilibrium nucleon emission,^{2,3} constrained to reproduce measured proton energy spectra and (${}^6\text{Li}, xn$)

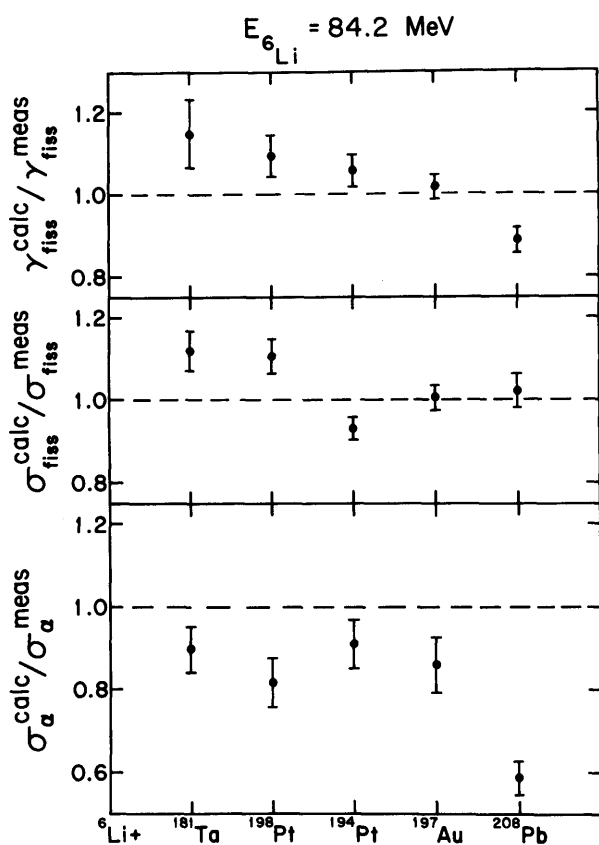


Figure 4. The ratio of calculated to measured values of σ_{α} , σ_{fiss} , and γ_{fiss} for ^6Li -induced fusion with five targets at 84.2 MeV bombarding energy when the calculations include both pre-equilibrium nucleon emission (see ref. 3) and the fadeout of the collective level density enhancement with increasing temperature. The collective cutoff deformation scaling parameter ζ has been adjusted to the value 1.05 to optimize the agreement between calculated and measured values of σ_{fiss} for 84.2 MeV $^6\text{Li} + ^{197}\text{Au}$. The error bars represent only the relative measurement uncertainties in σ_{α} , σ_{fiss} , and γ_{fiss} .

residue mass distributions) provide very good quantitative agreement with experimental results for σ_{fiss} , γ_{fiss} , and σ_{α} .

The calculations in Fig. 4 still employ pure RLDM-NIFG predictions for deformation energies, moments of inertia, and level densities. Our success with such

simple structure input is in contrast to reports^{5,7} that fission barriers at high angular momentum must be considerably reduced from RLDM values to account for heavy-ion induced fusion-fission measurements. In particular, we note a recent such report⁷ based on a conventional analysis of fusion and fission excitation functions for two entrance channels ($^{19}\text{F} + ^{181}\text{Ta}$ and $^{30}\text{Si} + ^{170}\text{Er}$) to the compound nucleus ^{200}Pb , which is precisely in the region we have studied. We intend to apply our complete calculations to these systems shortly, to see whether the discrepancy in conclusions can be attributed to the different level of sophistication in level density treatments, and to test our collective enhancement fade-out prescription, whose effects should vary significantly⁴ with the entrance-channel mass asymmetry.

- 1) S.E. Vigdor et al., Phys. Lett. 90B, 384 (1980).
- 2) S.E. Vigdor et al., IUCF Scientific and Technical Report 1980, p. 103.
- 3) S.E. Vigdor, in Proc. XIIIth Masurian Summer School on Nuclear Physics, Mikolajki, Poland, Sept. 1980, to be published in Nukleonika; S.E. Vigdor et al., IUCF preprint P-184 (submitted for publication in Phys. Rev. C).
- 4) S.E. Vigdor and H.J. Karwowski, IUCF preprint P-168 (submitted for publication in Phys. Rev. C).
- 5) M. Beckerman and M. Blann, Univ. of Rochester internal report UR-NSRL-135(1977), unpublished; M. Beckerman and M. Blann, Phys. Rev. C 17, 1615 (1978).
- 6) S. Bjornholm, A. Bohr, and B.R. Mottelson, Proc. Third Intl. Symp. on the Physics and Chemistry of Fission, Rochester, 1973 (Intl. Atomic Energy Agency, Vienna, 1974) Vol. I, p. 367; A. Bohr and B.R. Mottelson, Nuclear Structure, Vols. I and II (W.A. Benjamin, New York, 1969, and Reading, 1975).
- 7) J.R. Leigh et al., Phys. Rev. Lett. 48, 527 (1982), and references therein.